Aalborg University
DENMARK

Physical Model Tests on Spar Buoy for Offshore Floating Wind Energy Conversion

Users group H+ - DHI-09-SparBOFWEC

Tomasicchio, Giuseppe Roberto; Vicinanza, Diego; Belloli, Marco; Lugni, Claudio; Latham, John-Paul; Iglesias, Gregorio; Jensen, Bjarne; Vire, Axelle; Monbaliu, Jaak; Taruffi, Federico ; Pustina, Luca; Leone, Elisa; Russo, Sara; Francone, Antonio; Fontanella, Alessandro; Di Carlo, Simone; Muggiasca, Sara; Decorte, Griet ; Rivera-Arreba, Irene; Ferrante, Vincenzo; Battistella, Tommaso; Garcia, Raul Guanche; Díaz, Abel Martínez; Elsäßer, Björn; Via-Estrem, Lluis; Xiang, Jiansheng; Andersen, Morten Thøtt; Kofoed, Jens Peter; Kramer, Morten Bech

PHYSICAL MODEL TESTS ON SPAR BUOY FOR OFFSHORE FLOATING WIND ENERGY CONVERSION
Users group H+ - DHI-09-SparBOFWEC

Giuseppe Roberto Tomasicchio (1), Diego Vicinanza (2), Marco Belloli (3),
Claudio Lugni (4), John-Paul Latham (5), Gregorio Iglesias (6),
Bjarne Jensen (7), Axelle Vire (8), Jaak Monbaliu (9), Federico Taruffi (3), Luca Pustina (10), Elisa Leone (1), Sara Russo (2), Antonio Francone (11), Alessandro Fontanella (3), Simone Di Carlo (3), Sara Muggiasca (3), Griet Decorte (9), Irene Rivera-Arreba (8), Vincenzo Ferrante (2), Tommaso Battistella (12), Raul Guanche Garcia (12), Abel Martínez Díaz (6), Björn Elsäßer (7), Lluis Via-Estrem (5), Jiansheng Xiang (5), Morten Thøtt Andersen (13), Jens Peter Kofoed (13), Morten Bech Kramer (13),

(1) University of Salento, Italy, E-mail: roberto.tomasicchio@unisalento.it; elisa.leone@unisalento.it
(2) University of Campania, Italy, E-mail: diego.vicinanza@unicampania.it; ing.ferrante@gmail.com
(3) Polytechnic University of Milan, Italy, E-mail: marco.belloli@unimi.it; federico.taruffi@polimi.it; alessandro.fontanella@polimi.it; simone.dicarlo@mail.polimi.it; sara.muggiasca@polimi.it
(4) CNR (National Research Council), Italy, E-mail: claudio.lugni@cnr.it
(5) Imperial College London, England, E-mail: j.p.latham@imperial.ac.uk; j.xiang@imperial.ac.uk; l.via-estrem16@imperial.ac.uk
(6) University College Cork, Ireland, E-mail: gregorio.iglesias@ucc.ie; abel.martdiaz@gmail.com
(7) DHI Water & Environment, Denmark, E-mail: bjj@dhigroup.com; bje@dhigroup.com
(8) Delft University of Technology, Netherlands, E-mail: A.C.Vire@tudelft.nl; i.riveraarreba@tudelft.nl
(9) Catholic University of Leuven, Belgium, E-mail: jaak.monbaliu@kuleuven.be; griet.decorte@kuleuven.be
(10) Roma Tre University, Italy, E-mail: luca.pustina@uniroma3.it
(11) University of Calabria, Italy, E-mail: antonio.francone@unical.it
(12) University of Cantabria, Spain, E-mail: tommaso.battistella@unican.es; raul.guanche@unican.es
(13) Aalborg University, Denmark, E-mail: mta@civil.aau.dk; jpk@civil.aau.dk; mmk@civil.aau.dk

The present paper describes the experiences gained from the design methodology and operation of a 3D physical model experiment aimed to investigate the dynamic behaviour of a spar buoy (SB) off-shore floating wind turbine (WT) under different wind and wave conditions. The physical model tests have been performed at Danish Hydraulic Institute (DHI) off-shore wave basin within the European Union-Hydralab+ Initiative, in April 2019. The floating WT model has been subjected to a combination of regular and irregular wave attacks and wind loads.

1. INTRODUCTION

Nowadays, wind energy is said to account for 14% of Europe's total energy consumption, of which offshore wind has a share of 10% (WindEurope, 2019). This gives Europe a leading role in offshore wind energy. By moving offshore, wind energy gains many advantages compared to its onshore counterpart. Firstly, the social protest caused by visual pollution and noise is diminished and turbines can be made bigger. Secondly, at sea, winds are generally stronger and more stable which results in larger energy production. Due to new technologies, the turbines have increased in efficiency and so become viable from a financial point of view (Bilgili et al. 2011; Breton & Moe, 2009).

However, the added complexity due to the hostile offshore environment – waves, currents and salt – remains. Offshore wind has to cope especially with the severely limited installation depths of the commonly used bottom-founded structures, of which the majority are mono piles, which come relatively cheap, and gravity-based foundations. This is a major drawback as many densely populated areas worldwide are situated close to coastal areas characterized by huge wind

potential, but too large depths for conventional foundations to be built. This is especially the case for North-Western America, but European countries, e.g. Norway and Portugal, face this problem as well (Breton & Moe, 2009).

This unused energy potential could be harvested by founding the wind turbines on floating platforms, thus reducing the increasing cost induced by using bottom-founded substructures. Three platform types are currently being considered as viable options; (1) the tension-leg platform (TLP) which lends its stability to pre-tensioned mooring lines, (2) the spar-buoy (SB), which is stabilized by its large submerged volume and its deep-laying center of gravity, and (3) the semi-submersible (SS) which is stabilized by its large water plane area (Butterfield et al., 2007). Floating structures are already well established within the offshore industry. Especially, the SBs and the TLPs are frequently used in oil and gas applications.

Unfortunately, extrapolation to offshore wind applications is not justified, as the dynamic behavior of offshore wind turbines is radically different. The main differences are related to the slenderness of the wind turbine, the aero-elastic effects and the smaller submerged volumes, which increase the importance of viscous effects (Roald et al., 2013). Due to these differences, floating offshore wind turbines (FOWT) exhibit different behavior compared to their oil and gas ancestors. These differences need to be adequately assessed through lab testing in order to have sufficient understanding of the full-scale system as well as to validate numerical models for predicting this complex behavior.

Therefore, during this Hydralab+ project experiments were conducted on the spar-type floating offshore wind turbine. More specifically, these physical model tests were aimed at:

- to exploit the new large DHI wind-generator capable of generating wind speeds and to profit of the existence of the physical model from the Hydralab IV programme (Tomasicchio et al. 2017, 2018);
- to overcome most of the limitations from the adoption of an "approximate" systems to take into account the effect of the wind action when not in presence of a system to generate wind;
- investigating the coupling between a pitch-controlled rotor and the FOWT system rigid body hydrodynamics;
- create a reliable and accurate database for numerical modelling calibration and validation.

In the remainder of the present project DHI-09-SparBOFWEC, the physical model design of the FOWT will be discussed first. Next, the instrumentation is discussed and, subsequently, the test conditions are presented. To end with, conclusions are drawn and some future work based on these data is discussed.

2.   PHYSICAL MODEL DESIGN OF OFFSHORE FLOATING WT

The design of the FOWT model adopted during the Hydralab+ test campaign, shown in Figure 1, was based on the FOWT model developed as part of the OC3-Hywind (Offshore Code Comparison Collaboration) Phase IV project. The model consists of the NREL 5MW reference wind turbine (RWT) and the Hywind floating platform, a spar-buoy concept developed by Statoil of Norway. In the following, only the most relevant full-scale characteristics and their respective scaling used to define the scale model will be presented. For more details on the full-scale set-up, the reader is kindly referred to the NREL Technical Report (Jonkman, 2010). In the next paragraphs, the wind turbine and the rotor design, the spar-buoy platform and the mooring will be subsequently touched upon.

Wind turbine model
The NREL 5MW RWT is a typical utility-scale land and sea based multimegawatt wind turbine, suitable for deployment in deep waters (Jonkman et al., 2009). The turbine reaches the rated power of 5MW at 11.4 m/s and its operational phases are defined by a variable speed, collective pitch

controller. As described in the OC3-Hywind report (Jonkman, 2010), the tower base is connected to the spar-buoy at an elevation of 10 m above the sea water level (SWL). The height of the tower is 87.6 m above SWL and the hub is located at 90 m. Table 1 summarizes the main characteristics of the full-scale reference wind turbine.

Two main changes were done to the full-scale NREL 5MW RWT during the OC3-Hywind project. Contrary to the 6 m diameter of the NREL 5MW RWT, the tower base diameter equals the diameter of the upper part of the spar-buoy platform, which amounts to 6.5 m. Another difference between the baseline NREL 5MW wind turbine and the turbine mounted on the Hywind platform concerns the controller setup. Because the reactivity of the baseline turbine would introduce negative damping under operational loads, in the OC3-Hywind project, the gains of the PI pitch controller where reduced and the generator torque controller was switched from constant power to constant torque in operational conditions. Both adjustments were retained in the model of the FOWT system used in this test campaign.

The Hydralab+ wind turbine model was defined as a 1/40 Froude scale model of the NREL 5MW RWT. At present, the flexibility of the turbine tower is not considered and the tower is therefore considered as rigid. Some of the rotor dimensions were defined following the Froude scaling law as well. Although, in order to properly represent the rotor thrust response, the blade chord had to be scaled appropriately. The rotor is designed by upscaling the wind turbine model developed at Politecnico di Milano (PoliMi WTM), a 1/75 wind turbine model of the DTU 10MW RWT (Bak et al., 2013), designed and currently utilized for wind tunnel tests on FOWTs (Bayati et al., 2016; Bayati et al., 2017; Fontanella et al., 2018). The downscaled characteristics of the wind turbine tower and rotor-nacelle assembly are respectively shown in

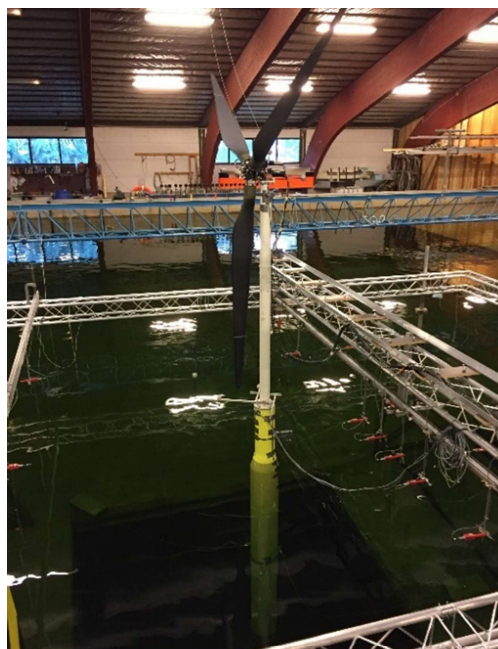Table *2* and

Table *3*.

Figure 1. Impression of the scaled spar-buoy wind turbine layout used during the Hydralab+ tests.

Aerodynamic properties of the rotor blades

Because the aerodynamic design of the rotor had to match the reference thrust and torque, the Hydralab+ rotor was designed as a geometrical upscale of the PoliMi WTM with its proper airfoil profiles. In order to improve the performance at low Reynolds numbers, which characterize the

airfoil aerodynamics for wind tunnel tests, the SD7032 airfoil was chosen in favour of the one applied for the NREL 5MW and the DTU 10MW.

Table 1. Full-scale properties of the baseline NREL 5MW wind turbine (Jonkman et al., 2009).

Rating	5 MW
Rotor Orientation, Configuration	Upwind, 3 Blades
Control	Variable Speed, Collective Pitch
Drivetrain	High Speed, Multiple-Stage Gearbox
Rotor, Hub Diameter	126 m, 3 m
Hub Height	90 m
Cut-In, Rated, Cut-Out Wind Speed	3 m/s, 11.4 m/s, 25 m/s
Cut-In, Rated Rotor Speed	6.9 rpm, 12.1 rpm
Rated Tip Speed	80 m/s
Overhang, Shaft Tilt, Precone	5 m, 5º, 2.5º
Rotor Mass	110000 kg
Nacelle Mass	240000 kg
Tower Mass	347460 kg
Coordinate Location of Overall CM	-0.2 m, 0.0 m, 64.0 m

Table 2. Downscaled properties of the NREL 5MW wind turbine.

HYDRALAB+ 1/40 model of NREL 5MW		λ_L=40 Froude
Length	[m]	1.86
Speed	[m/s]	6.325
Time	[s]	6.325
Frequency	[Hz]	0.158
Acceleration	[m/s^2]	1
Mass	[kg]	64000
Inertia	[kg.m^2]	1.02E8
Force	[N]	64000
Power	[W]	404771.5

Table 3. Downscaled properties of the rotor-nacelle assembly.

		NREL 5MW (Jonkman et al., 2009)	HYDRALAB
Rotor Orientation	[-]	Clockwise rotation - Upwind	Clockwise rotation - Upwind
Control	[-]	Variable speed - Collective Pitch	Variable speed - Collective Pitch
Number of blades	[-]	3	3
Rotor Diameter	[m]	126	3.15
Hub Diameter	[m]	3	0.075
Rated wind speed	[m/s]	11.4	1.8
Rotor speed (rated)	[rpm]	12.1	76.5
Ideal power (rated)	[W]	5.10^6	12.35

The blade section in the area near the blade root was determined through interpolation between this airfoil and a circular section, allowing for a smooth transition towards the blade root. The resulting airfoil is shown in Figure 2 and the original FFA airfoil is added to allow for comparison.

In order to determine the rotor blade shape, first, a blade shape in terms of twist and chord was determined by geometrically upscaling the PoliMi WTM blade shape. Subsequently, the aerodynamic performance of this rotor was assessed through numerical simulations using FAST v8 (an aero-hydro-servo-elastic tool for wind turbines developed by NREL) with the NREL 5MW RWT as target (Jonkman & Buhl, 2005). The resulting Hydralab+ blade and PoliMi WTM blade airfoil chords and blade twists are shown in
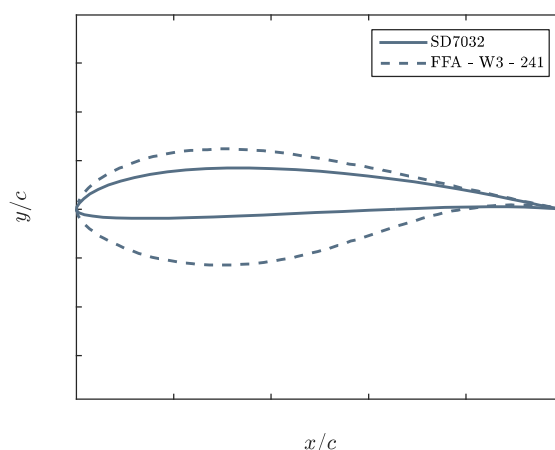
Figure 3.

Figure 2. Comparison between the SD7032 low thickness profile and the FFA profile in the full-scale wind turbine.

The 3-D surface of the blade was obtained by 3-D B-Spline interpolation from a 721-points cloud generated by the 193 blade sections. A CNC machined mold was realized based on the blade surface. The wind turbine model blades are fabricated in prepreg CFRP (carbon fiber reinforced plastic) through a vacuum bag oven process. A 3-D view of the blade surface is shown in **Errore. L'origine riferimento non è stata trovata.**.

The wind turbine model is equipped with a control and monitoring system and with actuators and sensors in order to ensure autonomous and continuous operation and to reproduce the reference full-scale turbine dynamics during experiments.

Four actuators characterize the mechatronics of the wind turbine model; a main shaft motor used to control the rotor angular speed and three dedicated motors allow to control the individual pitch angle of each blade in real-time. The wind turbine is also equipped with an encoder sensor measuring the generator speed used as controller feedback. An embedded system is able to control the actuators and acquire data from the sensors simultaneously.

The control system is designed based on the NREL 5MW, and the parameters are obtained applying the same scaling rules. The wind turbine controller resembles the standard variable-speed variable-pitch control strategy used by modern wind turbines to regulate power production and rotor speed throughout the machine operating range. Some modifications were introduced to the original controller to make the implementation on the scale model more effective (Fontanella et al., forthcoming).

The control strategy adopted is variable-speed variable-pitch. In this scheme, the turbine is programmed to operate at variable-speed and fixed-pitch below rated wind speed, to optimize the power extraction efficiency, and at variable pitch above rated wind speed, to regulate rotor speed and power.
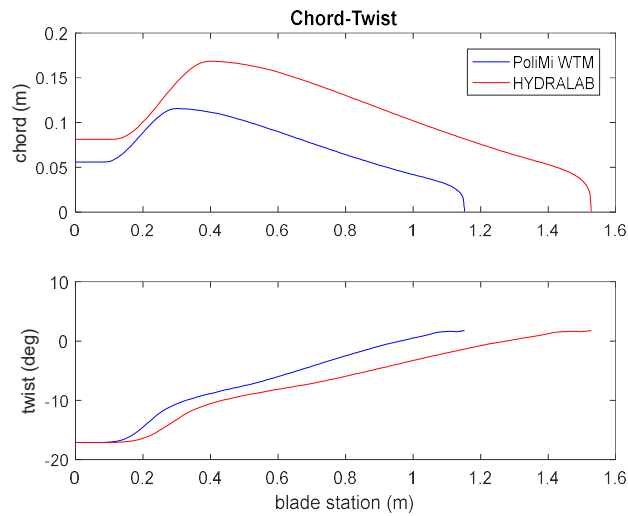
Figure 3. Dimensional chord and twist of the HYDRALAB model (red line) and the PoliMi WTM (blue line

The control system is characterized by three different regions of operation; (1) wind velocity range from start-up until cut-in speed, (2) the partial-load, operational velocity range in between cut-in and rated wind velocity – in this region the blade pitch is fixed at its minimum and the turbine is regulated at variable speed through the torque controller – , (3) the full-load, wind velocity range in between rated and cut-off wind velocity – in this region the generator torque is set at the rated value and the turbine operation is regulated by the blade pitch-to-feather PI controller.

The controller parameter set is obtained from the NREL 5MW coupled with the OC3-Hywind spar-buoy (Jonkman, 2010). The controller scheme is shown in Figure 4.

Hywind spar-buoy floating platform

The Hywind spar-buoy platform has a relatively simple geometry. The lower part of the platform has a diameter of 9.4 m. The upper part is tapered (between the depth of 4 and 12 m) in order to reach an upper part diameter of 6.5 m, which increases the transparency of the platform with respect to the hydrodynamic loads at the free surface. The main structural features of the Hywind platform are reported in Table 4. For additional information, the reader is referred to the OC3 report (Jonkman, 2010).

The OC3-Hywind spar-buoy platform scaling abides to a Froude similitude of 40. By doing so, both the geometry and the inertia between the scaled model and the full-scale structure where respected. The scaled down properties are given in Table 5, where the factor 1.025 takes into account the sea water.

Mooring system

Because the dimensions of the basin do not allow the full mooring lines to be modelled, the mooring line characteristics were approximated by a series of springs coupled to a mass placed at the bottom of the basin by an inelastic rope. The mass's and stiffness's of the various sections of the original mooring line were averaged in order to obtain the characteristics of a homogeneous mooring line. In designing the mooring, damping effects such as hydrodynamic drag and line-seabed drag were neglected (WindEurope, 2019). The scaled mooring system used in this project does not consider the yaw mooring rigidity and does not consider the damping related to hydrodynamic and friction effects. However, the system was modelled respecting the rigidity of the

6

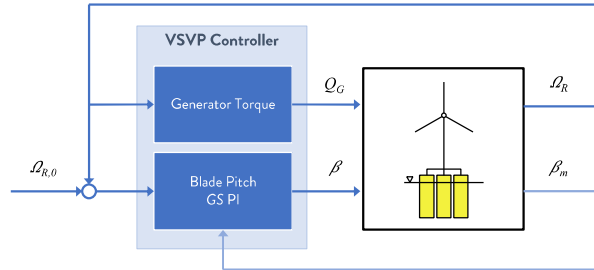more relevant platform degrees-of-freedom, such as the sway and surge. The mooring layout is shown in Figure 1.

Figure 4. VS-VP controller scheme.

Table 4. Geometrical properties of the OC3-Hywind spar buoy.

Total draft	120 m
Elevation to Platform Top (Tower Base) Above SWL	10 m
Depth to Top of Taper Below SWL	4 m
Depth to Bottom of Taper Below SWL	12 m
Platform Diameter Above Taper	6.5 m
Platform Diameter Below Taper	9.4 m
Platform Mass, Including Ballast	7466330 kg
CM Location Below SWL Along Platform Centerline	89.9155 m
Platform Roll Inertia about CM	4229230000 kg m^2
Platform Pitch Inertia about CM	4229230000 kg m^2
Platform Yaw Inertia about Platform Centerline	164230000 kg m^2

Table 5. Froude similitude scaling factors.

Magnitude	Ratio	Scale
Geometry	λ	40
Time	$\sqrt{\lambda}$	6.32
Velocity	$\sqrt{\lambda}$	6.32
Acceleration	1	1
Mass	1.025 λ^3	65600
Force	1.025 λ^3	65600
Pressure	1.025 λ	41
Reynolds Number	$\lambda^{1.5}$	253

3.   INSTRUMENTATION

The deep-water basin at DHI is 20m long, 30m wide and 3m deep, with a 3m x 3m and 6m deep pit at the mid of the basin. Its wave maker is equipped with 60 individually controlled flaps, which are able to generate regular and irregular unidirectional and directional wave fields. To minimize reflection, a 6.5m long sloping wave absorber is located opposite the wave maker. The free surface elevation is captured by a row of three wave gauges at 1.5m before the spar-buoy and a row of six wave gauges placed at 1m behind the spar-buoy. Both sets of wave gauges are placed perpendicular to the wave direction. In addition, two more wave gauges are located at the back of the spar-buoy to allow for an array reflection analysis to obtain the incident and reflected waves (Mansard & Funke, 1980). These wave gauges are placed parallel with respect to the wave propagation. The far-field layout of basin and the wave gauge locations in the near-field area close to the FOWT are shown in Figure 5.
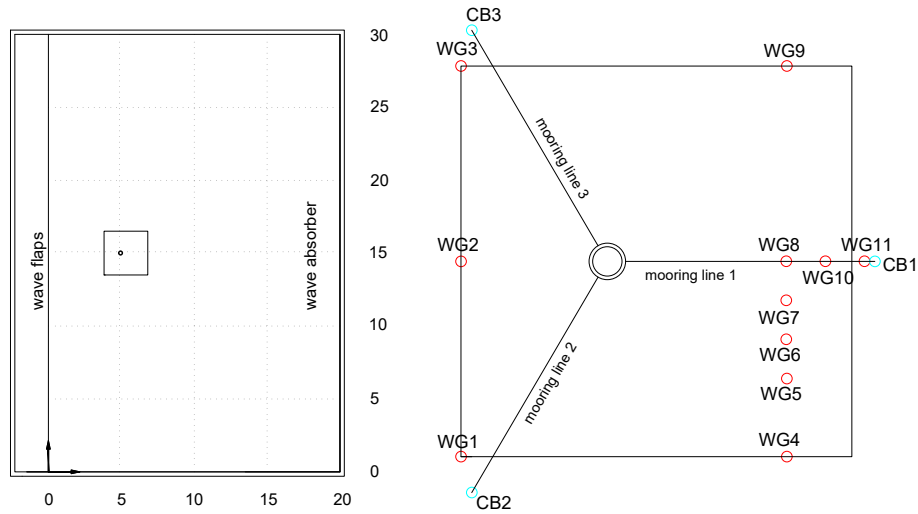
Figure 5. Wave basin layout (left) and wave gauge locations in the near-field area (right).

Wave elevation was sampled at 100Hz for regular and irregular waves. The duration for regular wave cases is about 3 minutes and 20-30 minutes for the irregular wave cases.

Furthermore, in case of large amplitude long waves, typically leading to Keulegan-Carpenter numbers larger than 7, vortex-shedding may occur in the small portion of the spar buoy just below the water level (Sumer & Fredsoe, 2006). In order to detect such vortex shedding effects, two Vectrino Acoustic Doppler Velocimeters were located close to each other at the back of the spar buoy. They were placed at an angle of 20 degrees with respect to the wave propagation.

To evaluate the vertical distribution of the dynamic pressures, three pressure transducers are located on the spar-buoy in the splash region. The wave impact forces are then obtained by spatially integrating these pressure measurements.

A Qualisys Tracking System was used to track the six-degrees-of-freedom motion of the FOWT. In addition, the model is equipped with four accelerometers. Two inertial frames measuring the translational and angular accelerations along three axes were used; one located at the top of the spar buoy and another one at the nacelle. Two uniaxial accelerometers were placed on the tower to capture the acceleration along the global x- and y-axis.

A load cell was placed at each mooring line connection to observe the tension force produced by the spar-buoy motion. An encoder placed in the wind turbine rotor allows measuring the angular velocity of the generator and, in addition, enables to track the reference for the blades' pitch. All observed data were synchronized by the DHI Wave Synthesizer.

4. PHYSICAL MODEL TEST CONDITIONS

Mmodel tests considered three conditions.: 1) the dynamic behaviour of the floating structure was investigated without wind conditions; 2) normal operational conditions have been simulated under combined rotation – rated wind speed conditions – and wave agitation; 3) extreme wave conditions were generated with the rotor stopped – cut-off wind speed. Preliminarily, a hammer test has been conducted in order to define the natural frequency of the tower.

Regular and irregular waves both orthogonal (0 degrees) and oblique (20 degrees) have been generated in presence of the floating structure composed by the spar buoy and the wind turbine. The selected wave conditions refer to typical storm conditions at both sea and ocean areas. In the following the characteristics of the adopted irregular wave attacks are given, where Hs and Tp represent the significant wave height and peak wave period (Table 6). Regular wave attacks

considered the following wave height values: 0.05 m, 0.13 m, and 0.25 m. To each of these values, the wave period was assumed ranging between 0.8 and 2.2 s.

Free decay tests have been performed in order to define the natural frequency for displacements and rotations and the total damping; they have been carried out combining different conditions in presence or absence of mooring lines and wind load.

Table 7. Adopted irregular wave characteristics for "no wind" and "above rated" conditions.

	Test #	Hs [m]	Tp [s]	DD	Wind speed (m/s)
NO WIND	1	0,08	1,53	0	0,00
	2	0,06	1,12		
	3	0,10	1,15		
	4	0,15	1,44		
	5	0,20	1,69		
	6	0,08	1,53	20	
	7	0,06	1,12		
	8	0,10	1,15		
	9	0,15	1,44		
	10	0,20	1,69		

	Test #	Hs [m]	Tp [s]	DD	Wind speed (m/s)
ABOVE RATED	11	0,08	1,53	0	1,84
	12	0,06	1,12		
	13	0,10	1,15		
	14	0,15	1,44		
	15	0,20	1,69		
	16	0,08	1,53	20	
	17	0,06	1,12		
	18	0,10	1,15		
	19	0,15	1,44		
	20	0,20	1,69		

5. EXPECTED FUTURE WORK

For organizational reasons, planning of the present project got a relevant delay which induced the User group H+-DHI-09-SparBOFWEC to enter the Lab in the 3rd week of March 2019 with expected end of the model tests on the 12th of April, well before the preparation of the present manuscript. Consequently, it would be too ambitious to give some conclusions. It is more realistic to say about the expected future common work.

The experimental data obtained during the Hydralab+ project will improve the understanding of the integrated floating wind turbine spar-buoy model, and will be used to validate numerical models, such as computational fluid dynamics models (CFD) to be adopted for accurate predictions of the aerodynamic and hydrodynamic performance of a spar-type floating offshore wind turbine.

ACKNOWLEDGEMENTS

REFERENCES

Bak, C., Zahle, F., Bitsche, R., Kim, T., Yde, A., Henriksen, L. C., Natarajan, A. (2013). The DTU 10-MW reference wind turbine. *Danish Wind Power Research 2013*.

Bayati, I., Belloli, M., Bernini, L., Fiore, E., Giberti, H., Zasso, A. (2016). On the functional design of the DTU 10MW wind turbine scale model of LIFES50+ project. *Journal of Physics: Conference Series*, *753*(5).

Bayati, I., Belloli, M., Bernini, L., Mikkelsen, R., Zasso, A. (2016). On the aero-elastic design of the DTU 10MW wind turbine blade for the LIFES50+ wind tunnel scale model. *Journal of Physics: Conference Series*, *753*(2).

Bayati, I., Belloli, M., Bernini, L., Zasso, A. (2017). Aerodynamic design methodology for wind tunnel tests of wind turbine rotors. *Journal of Wind Engineering and Industrial Aerodynamics*, *167*, 217-227.

Bilgili, M., Yasar, A., Simsek, E. (2011). Offshore wind power development in Europe and its comparison with onshore counterpart. *Renewable and Sustainable Energy Reviews., 15*(2)

Breton, S. and Moe, G. (2009). Status, plans and technologies for offshore wind turbines in Europe and North America. *Renewable Energy*, 34(3), 646-654.

Butterfield, S., Musial, W., Jonkman, J., Sclavounos, P. (2007). Engineering challenges for floating offshore wind turbines. *National Renewable Energy Lab (NREL)*, Golden, CO, USA.

Fontanella, A., Bayati, I., Belloli, M. (2018). Control of Floating Offshore Wind Turbines: Reduced-Order Modeling and Real-Time Implementation for Wind Tunnel Tests. In: ASME 2018 37th International Conference on Ocean, Offshore and Arctic Engineering.

Fontanella, A., Taruffi, F., Bayati, I., Belloli, M. (forthcoming) Variable-speed Variable-pitch control for a wind turbine scale model. *Energy procedia*.

Jonkman, J. M. and Buhl, M. L. (2005). FAST user's guide. *National Renewable Energy Laboratory (NREL)*. Golden, CO, USA.

Jonkman, J., Butterfield, S., Musial, W., Scott, G. (2009). Definition of a 5-MW reference wind turbine for offshore system development (No. NREL/TP-500-38060). *National Renewable Energy Lab (NREL)*. Golden, CO, USA.

Jonkman, J. (2010). Definition of the Floating System for Phase IV of OC3 (No. NREL/TP-500-47535). *National Renewable Energy Lab (NREL)*. Golden, CO, USA.

Mansard, E. and Funke, E. (1980). The measurement of incident and reflected spectra using a least squares method. *Proceedings of the 17th International Conference on Coastal Engineering*, (pp. 154-172). Sydney, Australia.

Roald, L., Jonkman, J., Robertson, A., Chokani, N. (2013). The effect of second-order hydrodynamics on floating offshore wind turbines. *Energy Procedia*, 35, 253-264.

Sumer, B. M. and Fredsoe, J. (2006). Hydrodynamics around cylindrical structures. *World Scientific Publishing Co.*

Tomasicchio, G.R., Avossa, A.M., Riefolo, L., Ricciardelli, F., Musci, E., D'Alessandro, F., Vicinanza, D. (2017). Dynamic modelling of a spar buoy wind turbine. Proceedings of the 36th International Conference on Ocean, Offshore and Arctic Engineering (OMAE2017)

Tomasicchio, G.R., D'Alessandro, F., Avossa A.M., Riefolo, L., Musci, E., Ricciardelli, F., Vicinanza, D. (2018). Experimental Modelling of the Dynamic Behaviour of a Spar Buoy Wind Turbine. Renewable Energy Journal, RENE-D-17-02232

WindEurope. (2019). Offshore Wind in Europe. Key trends and statistics 2018. Retrieved March 28, 2019, from https://windeurope.org/about-wind/statistics/european/wind-energy-in-europe-in-2018/.